Influence of the support composition on the hydrogenation of acrolein over Ag/SiO₂–Al₂O₃ catalysts

Claudia E. Volckmar [a], Michael Bron [a,1], Ursula Bentrup [b], Andreas Martin [b], Peter Claus [a,*]

[a] Department of Chemistry, Ernst-Berl-Institute/Chemical Technology II, Darmstadt University of Technology, Petersenstr. 20, D-64287 Darmstadt, Germany
[b] Leibniz-Institut für Katalyse e.V. an der Universität Rostock, Außenstelle Berlin, Richard-Willstätter-Str. 12, D-12489 Berlin

ARTICLE INFO

ABSTRACT

The gas phase hydrogenation of acrolein over supported silver catalysts has been investigated with a focus on the influence of the support acidity. Acidity has been varied by preparing silver catalysts supported on silica/alumina supports with varying SiO₂/Al₂O₃ ratio. After the catalytic experiments the Ag catalysts exhibit similar particle sizes, as revealed with TEM (transmission electron microscopy). The acidity of the samples was estimated using TPD of adsorbed ammonia which gives the total acidity of the samples, furthermore by IR of adsorbed pyridine to identify the Brønsted and Lewis acidity. No Brønsted acidity was found, and the Lewis acidity showed a clear dependence on the support composition. It is shown that a high total acidity and a high amount of strong Lewis acid sites on the catalysts cause a low conversion of acrolein and low selectivity to allyl alcohol. The interaction of silver with the support or effects of the metal–support perimeter are discussed as possible reasons for this behaviour.

© 2008 Published by Elsevier Inc.

1. Introduction

The production of allyl alcohol is of industrial interest because it is an important intermediate in the synthesis of allyl ethers and allyl esters as well as in the production of pharmaceutical products, fine chemicals and perfumes. Several approaches can be used to produce allyl alcohol, e.g. basic hydrolysis of allyl chloride, isomerisation of propylene oxide or saponification of allyl acetate. Furthermore, the gas phase hydrogenation of acrolein is also an option for the industrial production of allyl alcohol [1,2].

The use of typical hydrogenation catalysts like Pt, Pd, or Ni supported on non-reducible oxides leads mainly to the saturated aldehyde (reaction 1 in Fig. 1), which is understandable since thermodynamics and kinetics favour the hydrogenation of the C=C-bond over the C=O-bond [3].

The usage of supported silver as a hydrogenation catalyst resulted in a lowering of this disadvantageous course of the reaction and selectivities to allyl alcohol up to 44% [4–11] have been reached. Even higher selectivities of 75% [7,8] can be obtained over AgIn/support catalysts. Despite a possible industrial application of silver catalysts for the hydrogenation of acrolein, various studies have been performed by our group to elucidate the factors which govern the selectivities in this reaction over silver. In these stud-
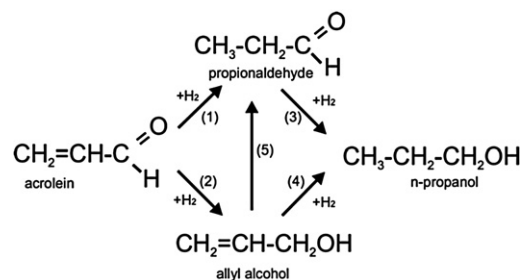

Fig. 1. Reaction network of the acrolein hydrogenation.

ies it was shown that the partial pressures of the reactants as well as the nanostructure of the catalysts have an influence on the selectivity towards the different products. For the formation of allyl alcohol a reaction pressure of at least 100 mbar is needed. Beyond this reaction pressure it is supposed that the adsorption geometry changes due to increasing coverage, leading to changes in hydrogenation selectivities. Small supported Ag particles favour the formation of allyl alcohol, which is likely related with the presence of electropositive sites like edges and kinks [4,5,10]. Defect site and subsurface oxygen have further been identified as an important factor influencing the selectivities in acrolein hydrogenation over silver [5,11,12]. These may especially be stabilised at the metal–support interface, making it possible to tune the catalytic properties by choosing an appropriate support material.

The goal of the present investigation is to determine the influence of the kind of support and the support acidity on the

Table 1
Composition of the support and the corresponding description for the catalysts used in this study.

SiO_2 content [%]	Al_2O_3 content [%]	Description of the catalyst
100	0	20Ag/SA100-P
80	20	20Ag/SA80-P
60	40	20Ag/SA60-P
40	60	20Ag/SA40-P
20	80	20Ag/SA20-P
0	100	20Ag/SA00-P

gas phase hydrogenation of acrolein over $Ag/SiO_2–Al_2O_3$ catalysts. From inorganic chemistry oxides of non-metals like SiO_2 are referred to as "acidic" oxides and oxides of metals are defined as "basic" oxides [13]. On one hand, the properties of the support material depend on the crystal chemical features of the bulk, on the other hand it also depends on the surface properties. Mixed oxides like silica/alumina contain covalent and ionic characteristics. Additional Brønsted acid sites are generated by bridging aluminium atoms. Our strategy was therefore to study the influence of support composition and acidity of $Ag/SiO_2–Al_2O_3$ catalysts with varying silica/alumina ratio to obtain catalysts with varying acidity.

2. Experimental

2.1. Catalyst preparation

Silver catalysts with a varying silica/alumina ratio were synthesised by co-precipitation [14,15]. Different silica/alumina ratios were used to obtain a variation of support acidity. A defined amount of $Al(NO_3)_3 \cdot 9H_2O$ (99.999%, Alfa Aesar) and $AgNO_3$ ($\geqslant$99.9%, Roth) was dissolved in distilled water. The amount of $AgNO_3$ was adjusted to yield 20 wt% of Ag in the final catalyst. This mixture was added to a 25% ammonia solution under stirring. Subsequently, a defined amount of 30 wt% silica-sol (Ludox AS-30 colloidal, Aldrich Co.) was added to the reaction mixture. The solvent was then evaporated in a water bath at 60 °C until a gel was obtained. Thereafter, the gel was dried in a vacuum oven at 110 °C for at least 12 h. The resulting solid was crushed to particles $\leqslant$500 μm and calcinated at 500 °C for 2 h in flowing air.

In Table 1 the nominal contents of silica and alumina of the different supports and the corresponding description of the catalysts are summarised.

2.2. Catalytic experiments

Catalytic experiments were performed in a computer-controlled tubular gas phase micro-reactor system, which has been described in detail elsewhere [16]. Directly before the catalytic measurement the catalysts were activated by in situ-reduction with hydrogen for 2 h at 325 °C. In this study the following reaction conditions were used: temperature $T = 250$ °C, total pressure $p_{total} = 1$ MPa, molar ratio hydrogen/acrolein = 20, $W/F_{AC,0} = 15.3$ g h mol^{-1}, with W as the weight of the catalyst and $F_{AC,0}$ as the molar flow of acrolein. In the course of the study the $W/F_{AC,0}$ ratio was varied, as specifically indicated in the text.

The effluent from the reactor is composed of acrolein and the reaction products shown in Fig. 1 as well as byproducts (lower hydrocarbons, oligomers) and was analysed on-line every 15 min by a gas chromatograph (HP 5890 series II) which was equipped with a flame ionisation detector and a 30 m J&W DB-WAX (polyethylene glycol: polar) capillary column. The reaction was carried out until steady state was reached and all selectivities reported in this publication are steady state values.

2.3. Catalyst characterisation

The catalysts were characterised by transmission electron microscopy (TEM) and BET surface area measurements. Analysis of the particle size distribution was performed by TEM using a JEM-3010, JOEL operating at 300 kV. Recording of the micrographs was done under the Scherzer focus condition. Subsequently, the software Digital Micrograph by GATAN was used to evaluate the particle size distribution from the TEM images and to calculate the average Ag particle size by sizing at least 300 particles.

The BET surface area was determined with a QUANTACHROME Adsorb-3B using nitrogen as probe gas.

Additionally, the acidity of the catalysts samples was investigated via temperature programmed desorption of adsorbed ammonia ("NH_3-TPD") and infrared spectroscopic investigation of the adsorption and desorption of pyridine ("pyridine-IR"). To measure the desorption spectra of the samples an AMI-1 (Altamira/Zeton) system was used. The NH_3 desorption experiments were conducted in flowing helium and desorbed NH_3 was detected with a thermal conductivity detector. The desorbed ammonia was absorbed in 0.05 N sulphuric acid and subsequently titrated with 0.05 N NaOH. "Tashiro-indicator," consisting of a solution of methyl red and methylene blue in ethanol with a transition at pH 5.4 was used for the titration.

Pyridine-IR was used to determine the different acid sites on the catalyst surface due to the fact that differently bonded pyridine gives specific absorption bands. Pyridine adsorbed at Lewis (L-Py) and Brønsted (PyH$^+$) acid sites exhibits bands at around 1445–1460 and 1540–1548 cm^{-1}, respectively. The bands of hydrogen-bonded pyridine (hb-Py) are in similar ranges of 1440–1447 and 1590–1600 cm^{-1} [13,17,18].

The spectra were recorded using a Bruker IFS 66 spectrometer equipped with a heatable and evacuable IR cell with CaF_2 windows, connected to a gas dosing-evacuating system. The powdered samples were pressed into self-supporting wafers with a diameter of 20 mm and a weight of 50 mg. Prior to pyridine adsorption, the samples were pretreated in flowing 5% H_2/Ar at 350 °C for 1 h followed by cooling to ambient temperature. Then, pyridine was adsorbed at this temperature for 1 h by bubbling an Ar stream through a pyridine-containing saturator. The physisorbed pyridine was removed by evacuating during 5 min at ambient temperature. The desorption of pyridine was followed by heating under vacuum up to 350 °C. The infrared spectra were recorded in transmission mode with 2 cm^{-1} resolution and 100 scans.

3. Results

3.1. Catalyst characterisation by TEM

Figs. 2 and 3 display post-mortem (i.e. after use in the catalytic reaction) TEM images and the particle size distributions of the samples 20Ag/SA100-P (Fig. 2) and 20Ag/SA80-P (Fig. 3). It can be seen, that the silver particles are well dispersed over the support material. From Fig. 3, left, we speculate, that the silver particles are in very close contact with the support and that it is partly encapsulated by the support. The same phenomenon was observed in a pronounced occurrence for Ag/TiO_2 catalyst systems [19,20]. However, at this point of research we can not provide further evidence for this speculation.

The particle size distribution in Fig. 2 of sample 20 Ag/SA100-P is very narrow in comparison to the sample 20 Ag/SA80-P which has a wider distribution in the range between 2 to 8 nm.

The average silver particle sizes of the various catalysts before and after the pre-treatment as well as after the catalytic experiments are summarised in Table 2.
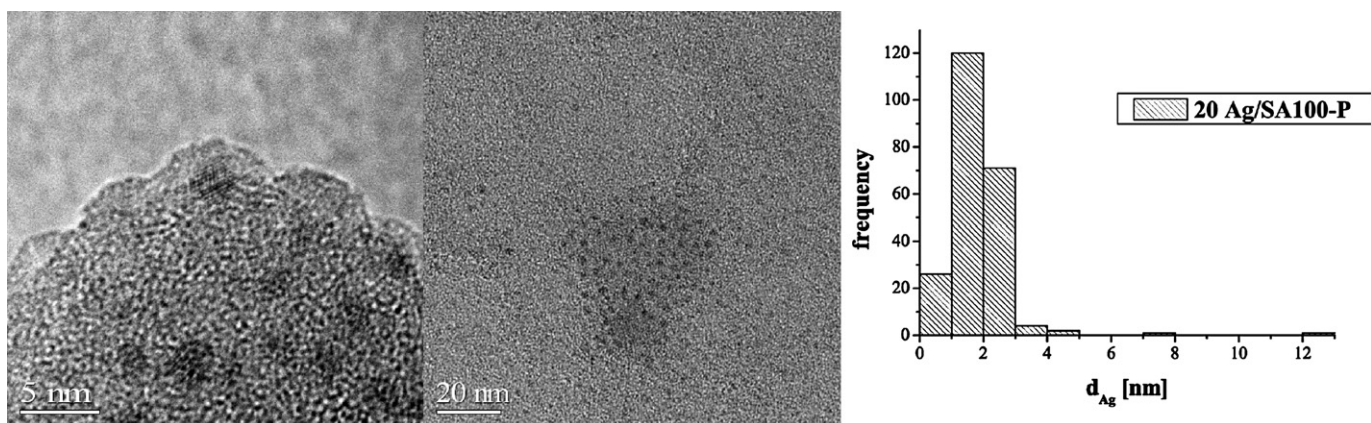
Fig. 2. TEM images of 20 Ag/SA100-P after reduction at 325 °C and catalysis at 250 °C in different magnifications and corresponding particles size distribution.
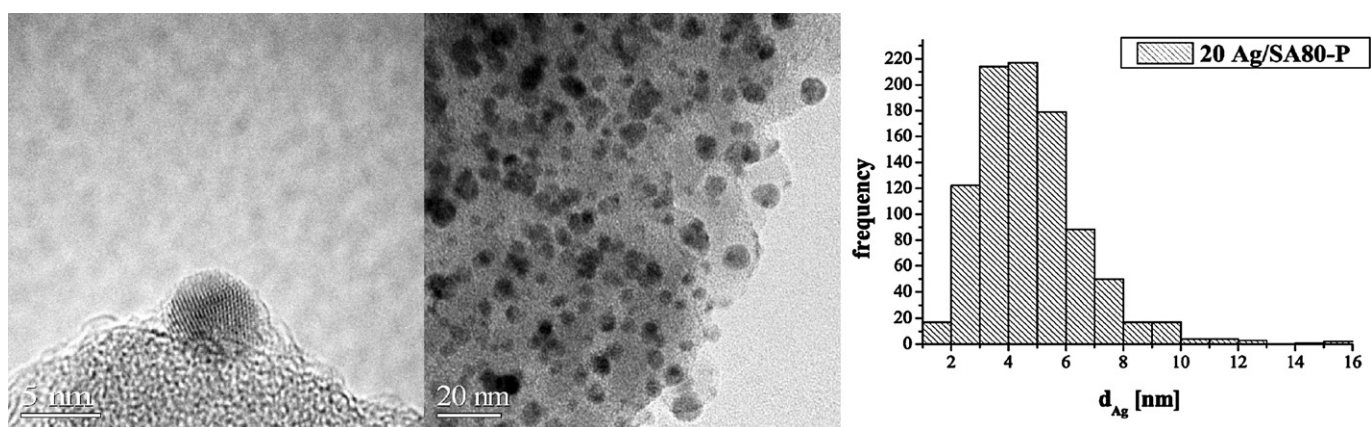

Fig. 3. TEM images of 20 Ag/SA80-P after reduction at 325 °C and catalysis at 250 °C in different magnifications and corresponding particle size distribution.

Table 2
Silver particle size of Ag/SiO$_2$–Al$_2$O$_3$ catalysts after calcination, after reduction and after the catalytic reaction as determined by TEM.

Catalyst	Al$_2$O$_3$ content in support [%]	d_{Ag} [nm] after		
		C500[a]	R325[b]	Catalysis[c]
20Ag/SA100-P	0	4.2 ± 2.5	6.6 ± 4.0	1.9 ± 1.0
20Ag/SA80-P	20	3.3 ± 2.9	7.6 ± 5.6	4.8 ± 1.9
20Ag/SA60-P	40	5.3 ± 2.3	5.3 ± 3.3	4.6 ± 1.9
20Ag/SA40-P	60	4.1 ± 2.8	3.6 ± 1.7	4.8 ± 4.6
20Ag/SA20-P	80	5.8 ± 2.5	3.3 ± 1.7	4.8 ± 2.7
20Ag/SA00-P	100	4.4 ± 2.5	7.7 ± 6.4	5.2 ± 2.7

[a] Calcination at 500 °C for 2 h in flowing air.
[b] Reduction at 325 °C for 2 h in flowing hydrogen.
[c] Catalytic reaction at 250 °C at a pressure of 1 MPa in hydrogen atmosphere.

The silver particles of the calcined samples are in the range of 3.3–5.8 nm. Subsequently, the calcined samples were reduced in flowing hydrogen at 325 °C, changing the range of the Ag particle sizes to 3.3–7.7 nm. There was no trend with the support composition recognisable. By treating the samples with hydrogen at elevated temperatures it is expected that oxidised Ag is reduced to Ag^0 which would simultaneously induce sintering of the Ag particles [21]. However, obviously this sintering also depends on the support material. The samples with an alumina content of 60 and 80% do not show a sintering of silver, but a re-dispersion. It is commonly known that a heat treatment of metal oxides in oxygen leads to a spreading of the oxide phase. The subsequent reduction at lower temperatures might cause a break-up of the particles into smaller ones [22]. Since Ag compounds are very sensitive against air it should be considered that the *reduced* catalysts, which have

been stored for several weeks or month, might have altered in air before they were investigated by TEM.

However, the Ag particle sizes after the catalytic reaction are all in the same range, except for the sample which contains only SiO$_2$ as support material. This leads to the assumption, that already a small amount of alumina in the support defines the characteristics of the support that influence the silver particle size during catalysis. The decrease in particle size due to catalysis for the Ag/SiO$_2$ catalyst is rather large. It has, however, to be kept in mind that silver catalysts in acrolein hydrogenation represent a very dynamic system, where catalyst surface oxidation by acrolein and subsequent re-reduction may occur [5,8,11], thus drastic changes of particles sizes under reaction conditions are not surprising. It has to be pointed out that the TEM images for the *used* catalysts, different than for the reduced ones, have been taken within one week after catalytic experiments, therefore we believe that changes in particle size due to storage in air are unlikely.

3.2. BET surface area

The specific BET surface area of the catalysts has been determined using nitrogen physisorption. The results are summarised in Table 3.

Increasing the alumina content in the support leads to an increase of the BET surface area of the catalysts. The samples SA80-P and SA20-P have been synthesised in a similar way as the Ag catalysts, however, without adding AgNO$_3$. The BET surface areas of these samples show the same trend as the Ag containing samples. Furthermore, the surface area of the Ag containing samples is only half the one of Ag free samples, indicating an influence of the sil-

Table 3
BET surface area of Ag/SiO$_2$–Al$_2$O$_3$ catalysts and Ag-free support materials.

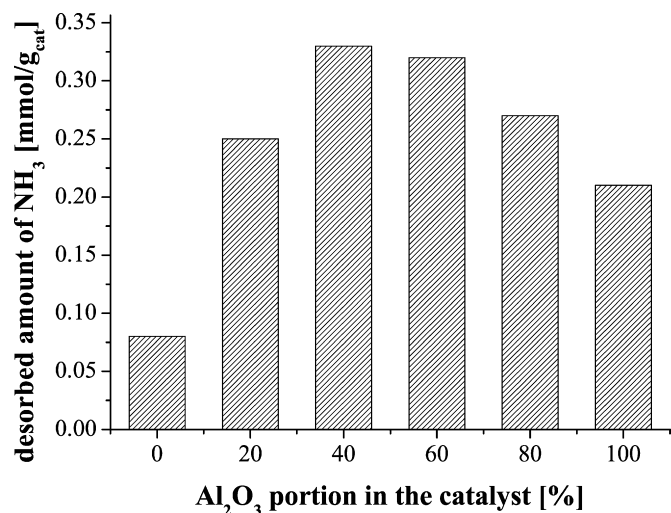| Catalysts	Al$_2$O$_3$ content in support [%]	BET [m^2/g]
20Ag/SA100-P	0	134
20Ag/SA80-P	20	152
20Ag/SA60-P	40	165
20Ag/SA40-P	60	175
20Ag/SA20-P	80	165
20Ag/SA00-P	100	211
SA80-P	20	249
SA20-P	80	290

Fig. 4. Total acidity of the Ag/SiO$_2$–Al$_2$O$_3$ catalysts in dependence of the alumina content in the support material as determined by NH$_3$-TPD.

ver on the condensation process. There is obviously not correlation of support surface area with Ag particle size (Table 2).

3.3. NH$_3$-temperature programmed desorption

The Ag precipitation catalysts were investigated via NH$_3$-TPD to determine the total acidity of the samples. Fig. 4 shows the des-orbed amount of ammonia plotted against the alumina content of the catalyst. At low alumina content the total acidity strongly increases with the alumina content, reaching a maximum at 40%. Further increase of the Al$_2$O$_3$ content in the catalysts leads to a decrease in total acidity.

3.4. Infrared spectroscopy of adsorbed pyridine

The adsorption of pyridine on the catalysts has been monitored with IR-spectroscopy in order to evaluate the relative amount of Lewis and Brønsted acid sites. The pyridine-IR spectra appeared to be rather noisy. Therefore, the evaluation of the results turned out to be more demanding than expected. It seems that the support materials of the prepared catalysts are amorphous since the Si–OH-bands are barely visible in the base spectra even with samples of high SiO$_2$ content. In Fig. 5 the spectra of pyridine adsorbed at the various samples are shown. The assignment of the various bands has been described above (see Section 2.3) and is given in the figure. As indicated the characteristic absorption bands, obtained at room temperature, of hydrogen-bonded pyridine are in similar range as the ones of pyridine adsorbed at Lewis and Brønsted acid sites. On this account, the discrimination of the Lewis acid sites from the spectra of adsorbed pyridine at room temperature is rather difficult due to an overlap of the absorption bands, which prohibits an exact assignment. Therefore, the thermal stability of the adsorbed pyridine species is utilised to identify the specific sites, due to the fact that at 200 °C the entire hydrogen-bonded pyridine is desorbed [17]. For this reason, spectra after pyridine desorption at different temperatures have been recorded as displayed in Fig. 6 for different Ag catalysts. In these spectra, a drastic decrease in intensity of the various bands can be seen with increasing temperature. The remaining bands can be attributed to pyridine adsorbed on Lewis acid sites. There was no pyridine adsorbed on Brønsted acid sites detectable in all the samples.

An estimation of the amount of Lewis acid sites is obtained by the determination of the integral band intensity around 1450 cm^{-1} at a temperature of 200 °C. The results are listed in Table 4. Bands at around 1600 cm^{-1} are also caused by pyridine adsorbed at Lewis acid sites and their position can be used to evaluate the strength of these sites. Compared with the Ag-free samples SA20-P and SA80-P, the Lewis sites of which are characterised by medium
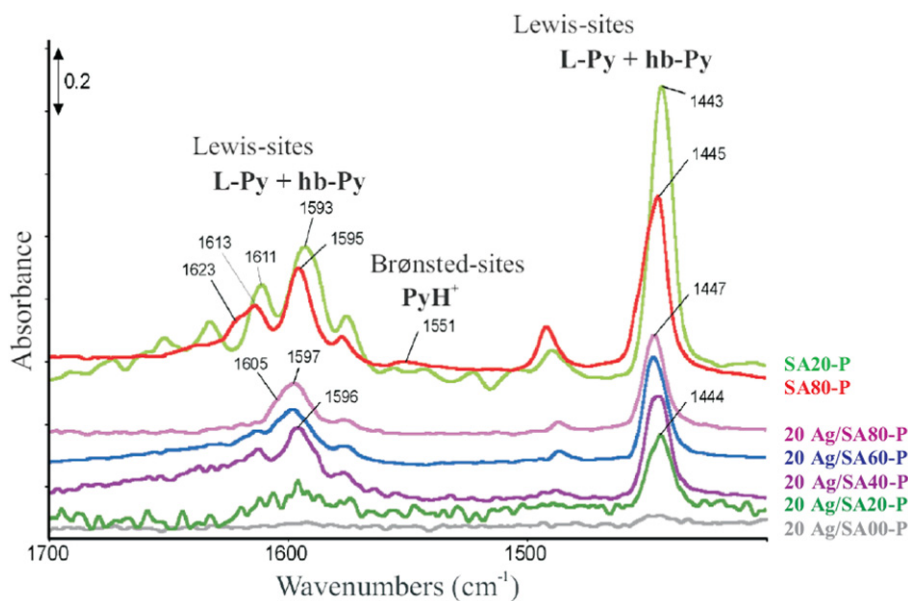

Fig. 5. IR spectra of adsorbed pyridine on various Ag/SiO$_2$–Al$_2$O$_3$ catalysts at ambient temperature.
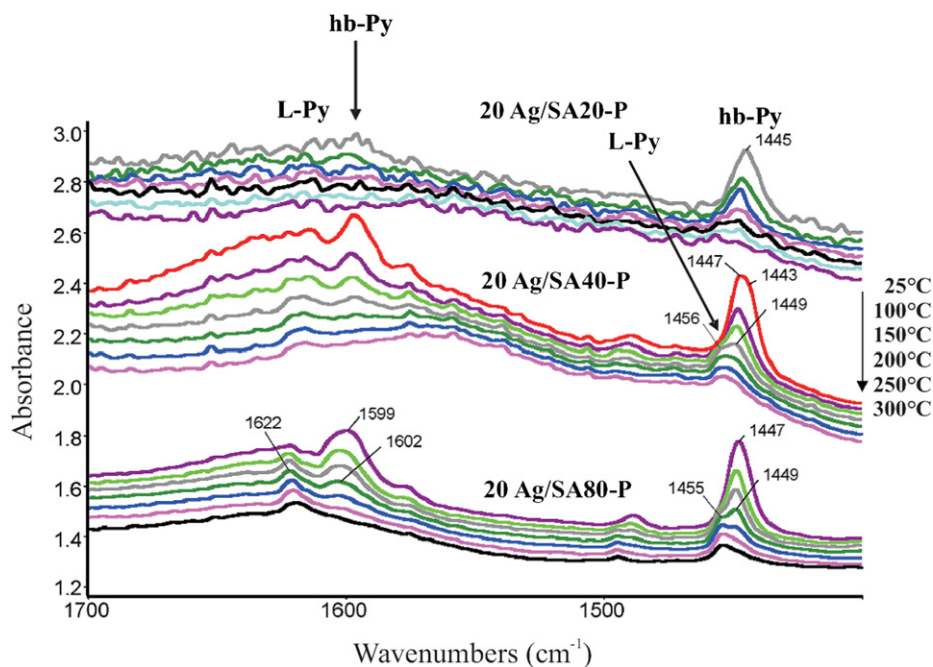
Fig. 6. IR spectra of pyridine desorption from 3 different $Ag/SiO_2-Al_2O_3$ catalysts. Each series measured at increasing temperatures as indicated.

Table 4
Integral band intensities of 20 $Ag/SiO_2-Al_2O_3$ catalysts at 200 °C measured via pyridine-IR.

Catalyst	20Ag/ SA100-P	20Ag/ SA80-P	20Ag/ SA60-P	20Ag/ SA40-P	20Ag/ SA20-P	20Ag/ SA00-P
Al_2O_3 content in support [%]	0	20	40	60	80	100
integral band intensity [a.u.]	–	1.8	2.0	2.0	1.4	0.3

(1593/1595 cm^{-1}) and strong (1613/1623 cm^{-1}) acidic Al^{3+} sites, the Ag samples obviously exhibit another type of medium-strong acidic sites (1596/1605 cm^{-1}). Related to the specific surface areas (cf. Table 3), the catalysts with a content of alumina in the range of 20–60% exhibit the highest Lewis acidity followed from the integral Lewis-band intensities summarised in Table 4. These samples also exhibit the highest total acidity.

3.5. Catalysis

The gas phase hydrogenation of acrolein has been carried out in a continuous flow reactor, as described in Section 2. The results of the catalytic investigation are summarised in Figs. 7 and 8. Conversion and selectivities are plotted against the alumina content in the catalyst. In Fig. 7 the modified residence time, W/F_{AC}, was constant for the individual experiments.

From Fig. 7 it can be seen that the activity increases with decreasing silica content in the support. The catalyst with the pure silica support is an exception and exhibits a rather high conversion. This seems, however, to be in agreement with the characterisation data since the Ag particle size is smaller compared to the other catalysts.

In order to compare the catalyst performance, especially the selectivities under identical conditions, additional hydrogenation
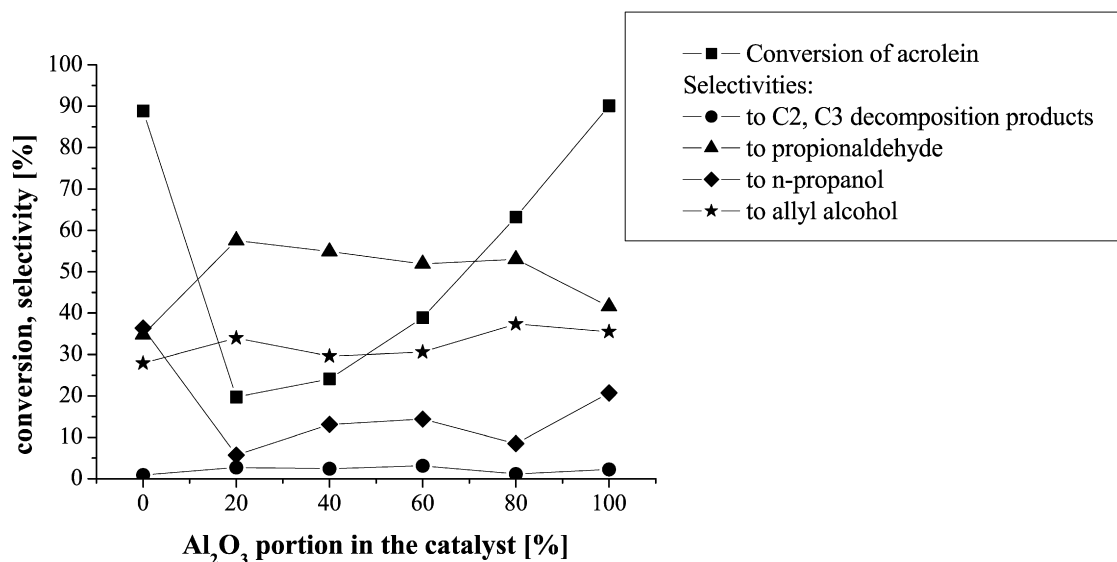

Fig. 7. Conversion and selectivity in acrolein hydrogenation over $Ag/SiO_2-Al_2O_3$ catalysts as a function of Al_2O_3 content in the support. $T_R = 250$ °C, $p = 1$ MPa, H_2:acrolein = 20:1.
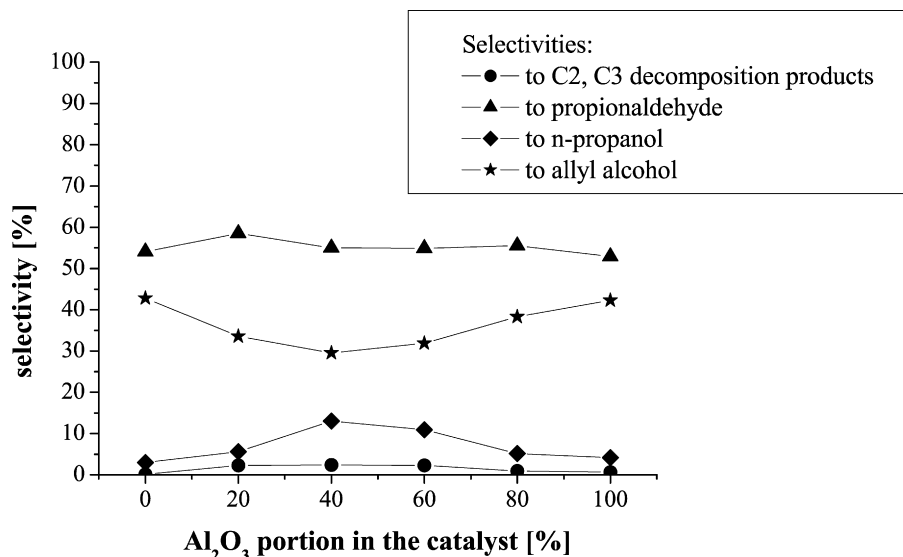
Fig. 8. Selectivity in acrolein hydrogenation vs Al_2O_3 content in Ag/SiO_2–Al_2O_3 catalysts at conversion of ∼25%. $T_R = 250\,°C$, $p = 1$ MPa, H_2:acrolein = 20:1.
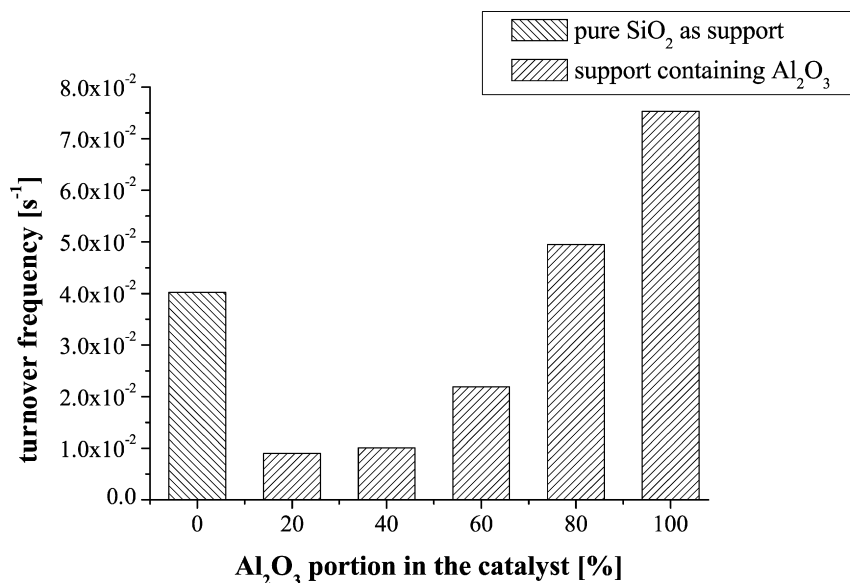

Fig. 9. Turnover frequencies in acrolein hydrogenation of Ag/SiO_2–Al_2O_3 catalysts.

experiments were performed at a conversion of 25% for all catalysts, which has been achieved by variation of W/F_{AC}.

Fig. 8 shows that the selectivity to allyl alcohol decreases with increasing content of alumina in the catalyst, reaching a minimum at 40% Al_2O_3 content. Simultaneously, the selectivity to n-propanol is rising, while the propionaldehyde selectivity remains nearly constant. At alumina contents larger than 60% the selectivity towards n-propanol is decreasing with a simultaneous increase of the selectivity towards allyl alcohol. The inverse dependence of allyl alcohol and n-propanol selectivity may indicate that n-propanol is mainly formed from allyl alcohol.

Additionally, the turnover frequencies (TOF) of the catalysts were estimated. For this, the number of surface atoms has been calculated by a mathematical model using average particle sizes. In this model it is assumed, that the Ag particles are built up of individual shells (onion-like structure) and that they retain their metallic character as well as their fcc-lattice under reaction conditions [23]. The latter assumption has been proven to be valid by in situ-EXAFS measurement for Ag/SiO_2 catalysts showing similar catalytic behaviour as those in the present study [8]. The calculated

dispersion of Ag on the surface of the catalysts was used to determine the TOF's of the different catalysts. In Fig. 9 the obtained TOF's are displayed against the portion of alumina in the support.

The TOF's increase with increasing alumina content in the support. The Ag particle sizes of the catalysts that contain alumina in the support are very similar, thus this increase in TOF should be due to the change in the properties of the support. However, since we can not exclude particle encapsulation, there may also be an error in estimation of free silver surface, influencing the calculation of the TOF.

4. Discussion

The results of the catalytic experiments and the characterisation measurements are complied in Table 5. On the basis of the similar silver particle sizes of the catalysts after reaction, except for Ag supported on pure SiO_2 (Table 2), it was possible to exclude the dependence of the selectivity in acrolein hydrogenation on the silver particle size of the samples. Therefore, the catalyst performance could be associated with the different support properties.

Table 5
Catalytic properties in acrolein hydrogenation and support acidity of Ag/SiO$_2$–Al$_2$O$_3$ catalysts.

Catalyst[a]	20Ag/ SA100-P	20Ag/ SA80-P	20Ag/ SA60-P	20Ag/ SA40-P	20Ag/ SA20-P	20Ag/ SA00-P
Al$_2$O$_3$ content in support [%]	0	20	40	60	80	100
Acidity[b] [10^{-3} mmol/m^2]	0.6	1.64	2.0	1.83	1.64	1.0
Conversion[c] [%]	89	20	24	39	63	90
Selectivity[d] [%]	43	34	29	32	38	42
Yield[e] [%]	25	7	7	12	24	32

[a] Amount of Ag = 20 wt%.
[b] Desorbed amount of NH$_3$ referred to the BET surface.
[c] $W/F_{AC,0} = 15.3$ g h/mol.
[d] Selectivity to allyl alcohol with X = const. (25%).
[e] Allyl alcohol.

A comparison of the catalysts at the same conversion of 25% (Fig. 8) showed that the samples with no or very high Al$_2$O$_3$ content in the support showed selectivity patterns, which are commonly observed in acrolein hydrogenation over supported silver nanoparticles at high pressure [4,5,9,19]. The selectivity to allyl alcohol is approx. 40%, and the extent of consecutive reactions as well as the formation of by-products is rather low. These samples are characterised by their low amount and decreased strength of Lewis acid sites. The observation of a catalytic behaviour similar to that of other Ag/support catalysts indicates, that the special preparation procedure in the present case does not influence the catalytic behaviour. However, for the catalysts with medium alumina content (i.e., 40 or 60%), the selectivity to *n*-propanol becomes significant. At the same time, the selectivity to allyl alcohol decreases, indicating that allyl alcohol formation and *n*-propanol formation are related to each other. Consecutive reaction might either occur by re-adsorbed allyl alcohol, which is then further hydrogenated, or, more likely, further reaction of adsorbed semi-hydrogenated intermediates. From Table 5 it can be seen that a maximum of total acidity related to the BET surface was reached for 20Ag/SA60-P and 20Ag/SA40-P with an alumina content of 40% and 60%, respectively, which are exactly the catalysts that achieved the lowest selectivity to the desired unsaturated alcohol or the highest amount of consecutive reaction.

The results of pyridine-IR showed a similar trend of the Lewis acidity as the results for the total acidity measured by NH$_3$-TPD. However, it has to be mentioned that the strongest Lewis acid sites were achieved for 20Ag/SA80-P, 20Ag/SA60-P and 20Ag/SA40-P. These samples also reached the lowest TOFs as well as the lowest yields for allyl alcohol of all the samples. Thus, it can be concluded that the amount and strength of the Lewis acid sites of the support material strongly influence the catalytic performance of the catalysts with regard to selectivity and, probably, activity. If the number and the strength of the Lewis acid sites decrease then an increase of the yield for allyl alcohol and the TOF is obtained. It is worth to mention that all Ag/SiO$_2$–Al$_2$O$_3$ catalysts had in common that there were no Brønsted acid sites detectable at the surface. Therefore, the acidity of the different samples achieved lower values than the acidity of crystalline zeolite samples which contain OH-groups on their surfaces which act as Brønsted acid sites [24].

Various mechanisms can be considered, in which the support influences the catalytic properties of the deposited metal. While different particle sizes stabilised by the different support materials can be excluded from our TEM measurements, it may be that the shape of the particles is different on the various support materials. However, on one hand the differences in catalytic behaviour is too large to be only due to particle shape effects, and from the available TEM images there is no hint on dominating particle shapes or differences. Such indirect structural effects by the support can thus be excluded.

A second possibility would be a direct participation of the support material in the catalytic reaction. Special active sites might form at the metal–support perimeter, which might be able to coordinate and activate different functional groups of the acrolein molecule. The exchange of OH-groups of silica with deuterium to form O–D, which was shown recently [4,11], was faster in the presence of silver nanoparticles. This also indicates the strong influence of the metal–support perimeter and thus the kind of support material on the activity of silver hydrogenation catalysts [19]. We recently were able to show, that silver, which in its pure form interacts only very weakly with hydrogen, needs positively charged sites induced by subsurface oxygen or defects, which might be stabilised at the metal–support perimeter to be able to dissociate hydrogen and to be an active hydrogenation catalyst [5,11]. However, while such influences can not be excluded, it has to be stated that the catalytic properties correlate with the acidity of the support, and not with its composition.

At this point, it is worthwhile to highlight some results from literature: Hájek and Murzin [25] experienced an increase in activity in the cinnamaldehyde hydrogenation over Pt modified molecular sieves with increased support acidity. They also experienced a simultaneously decrease of selectivity towards the unsaturated alcohol. Similar results were obtained by the authors over Ru/Al$_2$O$_3$ catalysts [26]. The support material plays an important role in this process since the adsorption strength of the different compounds is changed by the different supports. The group of Koningsberger found, that the hydrogen chemisorption properties of supported metal particles depends on the support ionicity or acid/base properties, however, they investigated much smaller particles then those used in our studies [27–31]. A dependency of Lewis acidity on the activity of metal catalysts supported on silica/alumina with varied SiO$_2$/Al$_2$O$_3$ ratio was also found by Yasuda et al. [32] and Venezia et al. [33]. Reschetilowski et al. [34,35] explained metal–support interaction of catalysts with varying support acidity by the HSAB concept of Pearson [36] (HSAB: hard and soft acids and bases). The authors observed an activity loss in hydrogenolysis and isomerisation reactions with increasing support acidity [34,35].

From these studies it is clear that the acidity of the support might be a possible explanation for the selectivity patterns that were observed in the present study. Having in mind that the silver particles of our catalysts are in strong contact with the support and probably partly encapsulated, it might be that the interaction of the metal with the Lewis acid sites of the support leads to a change in the hydrogenation properties of the silver by influencing hydrogen adsorption properties/coverage as well as acrolein adsorption. This would in principle be an electronic interaction, which is usually observed on smaller particles as those found in this study. On the other hand, the striking correlation between acidity and catalytic properties calls for an explanation of the observed behaviour, which goes beyond pure effects of support composition.

5. Conclusion

Using the precipitation method for catalyst preparation led to supported silver catalysts with varying SiO$_2$/Al$_2$O$_3$ ratio but almost equal Ag particle size. Changes in activity and selectivity could be ascribed to the varying support properties of the catalysts which were investigated by several characterisation methods.

From pyridine-IR and NH$_3$-TPD it results, that the highest amount of Lewis acid sites as well as the highest total acidity are achieved at a medium Al$_2$O$_3$ content. These samples exhibit the lowest selectivity to allyl alcohol. The strongest Lewis acid sites were found at low and medium Al$_2$O$_3$ content. These samples also obtained a low TOF and a low yield of allyl alcohol so that it is concluded that these strong Lewis acid sites have a significant influence on the catalytic performance of the catalysts. Increasing

the Al_2O_3 content in the support leads to a decrease of the total acidity and the strong Lewis acid sites seem to disappear.

While influences of the metal–support interface can not be excluded, it is suggested that the interaction of silver particles with the more or less acid support materials influences their catalytic behaviour, leading to the observed variation in selectivity and activity.

Acknowledgments

References

[1] H.-J. Arpe, Industrielle Organische Chemie, 6 ed., Wiley–VCH, Weinheim, 2007, p. 330.
[2] W. Foerst, in: Ulmanns Encyklopädie der Technischen Chemie, vol. 3, 3 ed., Urban & Schwarzberg, München/Berlin, 1953, p. 315.
[3] P. Claus, Top. Catal. 5 (1998) 51–62.
[4] M. Bron, E. Kondratenko, A. Trunschke, P. Claus, Z. Phys. Chem. 218 (2004) 405.
[5] M. Bron, D. Teschner, A. Knop-Gericke, F. Jentoft, J. Hohmeyer, C. Volckmar, B. Steinhauer, R. Schlögl, P. Claus, Phys. Chem. Chem. Phys. 9 (2007) 3559.
[6] J. Hohmeyer, E. Kondratenko, M. Bron, J. Kröhnert, B. Steinhauer, C. Volckmar, F.C. Jentoft, R. Schlögl, P. Claus, in preparation.
[7] M. Lucas, P. Claus, Chem. Ing. Tech. 77 (2005) 110.
[8] F. Haass, M. Bron, H. Fuess, P. Claus, Appl. Catal. A 318 (2007) 9.
[9] M. Bron, D. Teschner, A. Knop-Gericke, B. Steinhauer, A. Scheybal, M. Hävecker, D. Wang, R. Födisch, D. Hönicke, A. Wootsch, R. Schlögl, P. Claus, J. Catal. 234 (2005) 37.
[10] M. Bron, D. Teschner, A. Knop-Gericke, A. Scheybal, B. Steinhauer, M. Hävecker, R. Födisch, D. Hönicke, R. Schlögl, P. Claus, Catal. Commun. 6 (2005) 371.
[11] M. Bron, D. Teschner, U. Wild, B. Steinhauer, A. Knop-Gericke, C. Volckmar, A. Wootsch, R. Schlögl, P. Claus, Appl. Catal. A 341 (2008) 127.
[12] A.B. Mohammad, I.V. Yudanov, K.H. Lim, K.M. Neyman, N. Rösch, J. Phys. Chem. C 112 (2008) 1628.
[13] G. Busca, Phys. Chem. Chem. Phys. 1 (1999) 723.
[14] Y. Nagase, T. Takahashi, K. Hirabayashi, Ibaraki Daigaku Kogakubu Shuko 40 (1992) 221.
[15] Y. Nagase, Ibaraki Daigaku Kogakubu Shuko 39 (1991) 165.
[16] M. Lucas, P. Claus, Chem. Ing. Tech. 67 (1995) 773.
[17] V.N. Kalevaru, A. Benhmid, J. Radnik, M.-M. Pohl, U. Bentrup, A. Martin, J. Catal. 246 (2007) 399.
[18] G. Busca, Catal. Today 41 (1998) 191.
[19] W. Grünert, A. Brückner, H. Hofmeister, P. Claus, J. Phys. Chem. B 108 (2004) 5709.
[20] P. Claus, H. Hofmeister, J. Phys. Chem. B 103 (1999) 2766.
[21] J.K. Plischke, M.A. Vannice, Appl. Catal. 42 (1988) 255.
[22] Z. Qu, W. Huang, M. Cheng, X. Bao, J. Phys. Chem. B 109 (2005) 15842.
[23] J.M. Montejano-Carrizales, F. Anguilera-Granja, J.L. Morán-López, Nanostruct. Mater. 8 (1997) 269.
[24] A. Corma, Chem. Rev. 97 (1997) 2373.
[25] J. Hájek, N. Kumar, D. Francová, I. Paseka, P. Mäki-Arvela, T. Salmi, D.Y. Murzin, Chem. Eng. Technol. 27 (2004) 1290–1295.
[26] P. Mäki-Arvela, J. Hájek, T. Salmi, D.Yu. Murzin, Appl. Catal. A 292 (2005) 1.
[27] Y. Ji, A.M.J. van der Eerden, V. Koot, P.J. Kooyman, J.D. Meeldijk, B.M. Weckhuysen, D.C. Koningsberger, J. Catal. 234 (2005) 376.
[28] M.K. Oudenhuijzen, J.A. van Bokhoven, D.E. Ramaker, D.C. Koningsberger, J. Phys. Chem. B 108 (2004) 20247.
[29] M.K. Oudenhuijzen, J.A. van Bokhoven, J.T. Miller, D.E. Ramaker, D.C. Koningsberger, J. Am. Chem. Soc. 127 (2005) 1530.
[30] M.K. Oudenhuijzen, J.H. Bitter, D.C. Koningsberger, J. Phys. Chem. B 105 (2001) 4616.
[31] D.C. Koningsberger, D.E. Ramaker, J.T. Miller, J. de Graaf, B.L. Mojet, Top. Catal. 15 (2001) 35.
[32] H. Yasuda, T. Sato, Y. Yoshimura, Catal. Today 50 (1999) 63.
[33] A.M. Venezia, V. La Parola, B. Pawelec, J.L.G. Fierro, Appl. Catal. A 264 (2004) 43.
[34] W. Reschetilowski, K.-P. Wendlandt, Wissenschaftliche Zeitschrift TH Leuna-Merseburg 31 (1989) 186.
[35] W. Reschetilowski, Dissertation B, TH "Carl Schorlemmer" Leuna-Merseburg, Merseburg, 1986.
[36] R.G. Pearson, J. Am. Chem. Soc. 85 (1963) 3533.